2021 IEEE 34th International Conference on Micro Electro Mechanical Systems (MEMS) | 978-1-6654-1912-3/20/$31.00 ©2021 IEEE | DOI: 10.1109/MEMS51782.2021.9375415

DOUBLE-SIDED LASER-INDUCED GRAPHENE BASED SMART BRACELET FOR SENSING AND ENERGY

Haobin Wang[1], Zehua Xiang[1], Ji Wan[1], Yu Song[1], and Haixia Zhang[1,2,]*
[1]National Key Laboratory of Science and Technology on Micro/Nano Fabrication, Institute of Microelectronics, Peking University, Beijing, CHINA
[2]Academy for Advanced Interdisciplinary Studies, Peking University, Beijing, CHINA

ABSTRACT

For addressing the issue of power consumption and integration level of wearable electronics, this work proposes a smart bracelet based on double-sided laser-induced graphene (LIG) technology both for sensing and energy. Benefiting from the high conductivity of the LIG, the LIG-based triboelectric nanogenerator (LIG-TENG) on the inner side of the bracelet can efficiently convert human kinetic energy into active signals and pulsed electricity. Meanwhile, the micro-supercapacitors (MSCs) on the outer side take advantage of the high surface area of LIG and in-situ store the energy collected by LIG-TENG. Furthermore, the via assisted by unlased polyimide (PI) with optimized parameters realizes valid interconnection and avoids complicated wiring. This smart system in versatile and facile process exhibits great potential in diversified functional requirements.

KEYWORDS

double-sided, laser-induced graphene, triboelectric nanogenerators, micro-supercapacitors, active sensing, self-charging unit

INTRODUCTION

With the rapid flourishment of mobile terminals, portable/wearable electronics [1-3] and daily health monitoring/management [4-6], the further reduction of device power consumption and real-time signal extraction are urgently required. The daily movements of human body actually contain a wealth of kinetic energy [7-9] and rich valuable information [10-12], which are often overlooked due to the failure to select proper transduction mechanism or wearable configuration.

Triboelectric nanogenerators (TENGs) play a huge advantage in low-frequency energy conversion and form real-time high voltage outputs [13, 14]. In order to realize the synergy of physiological signal sensing and motion energy capturing in on-body scenarios, the configuration design and manufacturing process of TENGs need to be further developed.

Besides, while pursuing the performance integration of wearable systems, it is particularly important to consider more factors to achieve a higher integration level. With respect to the fabrication process, assembling TENGs and energy storage devices (such as micro-supercapacitors (MSCs)) with compatible processes into self-charging power units (SCPUs) is an effective approach to make systems more compact and portable [4, 15, 16].

Herein, we put forward a smart bracelet all based on the laser-induced graphene (LIG) process. The good electrical conductivity and high surface area contribute to the high performance of TENG and MSCs, respectively. Additionally, we develop a double-sided processing and via interconnection technology with optimized parameters, which greatly improves the integration level. This system provides important guidance for signal detection and energy supply of wearable electronics.

EXPERIMENTAL METHODS

Fabrication of LIG electrodes

The electrodes of two major components of the system, TENG and MSCs, are both fabricated by a single-step programmable laser direct writing process. LIG electrodes are synthesized by irradiation of 75 μm polyimide (PI) sheets (considering the overall flexibility of the system and the feasibility of the double-sided processing) with a 10.6 μm CO_2 infrared laser (Voiern Laser Technology Co., Ltd.) at a scan rate of 90 mm s^{-1}, minimum power of 7.7%, and maximum power of 9.5%. As shown in Fig. 1(a), the electrode processing areas on the both side of bracelet are about 20 cm × 3.5 cm, which are well aligned with reference marks.

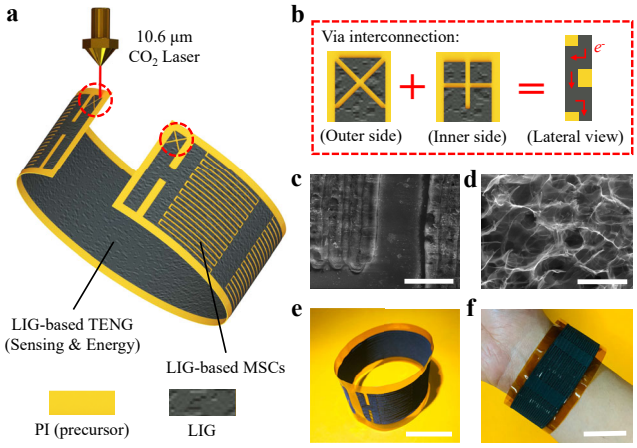

***Figure 1**: (a) Processing diagram of the smart bracelet. (b) Schematic diagram of the via interconnection. (c-d) SEM and (e-f) Optical images of the prepared device. Scale bars: (c) 500 μm, (d) 5 μm, (e-f) 2 cm.*

Fabrication of LIG-based TENG (LIG-TENG)

The single-electrode TENG can be easily fabricated by depositing/attaching friction layer material on the as-formed inner LIG electrode. The friction material can be selected according to the actual needs. It should be noted that the reserved positions are needed for the pins of the rectifier bridge and the interconnection with the MSCs.

Fabrication of LIG-based MSCs (LIG-MSCs)

The electrolytes for MSCs can also be selected on demand. The electrolytes in this work is prepared by adding polyvinyl alcohol (PVA) powder (5 g) into H_3PO_4, aqueous solution (5 g H_3PO_4 into 50 ml deionized water). The whole

mixture is heated to 85 ℃ under vigorous stirring until the solution becomes clear. The corresponding positions on the outer side of the bracelet are also required to be reserved.

Fabrication of via interconnection

Increasing the laser-induced power at the previously reserved positions makes the double-sided LIG penetrate through to form vias. To ensure the reliability of interconnection, the unlased PI lattices in Fig. 1(b) reinforce the LIG vias. Besides, the staggered complementary design of lattices considers the conductivity of the vias at the same time.

Measurement and Analysis

The morphologies of LIG layer are observed using a scanning electron microscope (SEM) (Quanta 600F, FEI Co.). A digital oscilloscope (Agilent DSO-X 2014A) is adopted to test the voltage outputs of LIG-TENG and the self-charging capability of the smart bracelet. The current outputs of LIG-TENG are amplified by an SR570 low-noise current amplifier. All of the electrochemical tests of the LIG-MSCs are carried out by a CHI660C (CH instrument) electrochemical workstation.

RESULTS AND DISCUSSION

SEM and Optical analysis

The SEM image in Fig. 1(c) clearly depicts the neat-edge of LIG-MSCs' interdigital electrodes fabricated under suitable processing parameters, which is critical to their electrochemical performance. While the temperature is above 2500 ℃ under laser exposure, the rapid outgassing of non-carbon elements allows the LIG for a porous microstructure and high surface area [17], which is confirmed by Fig. 1(d). Figure 1(e-f) portray the flexibility and wearability of the as-formed bracelet, which also shows the uniformity of large area processing.

Controllability and Reliability analysis of processing

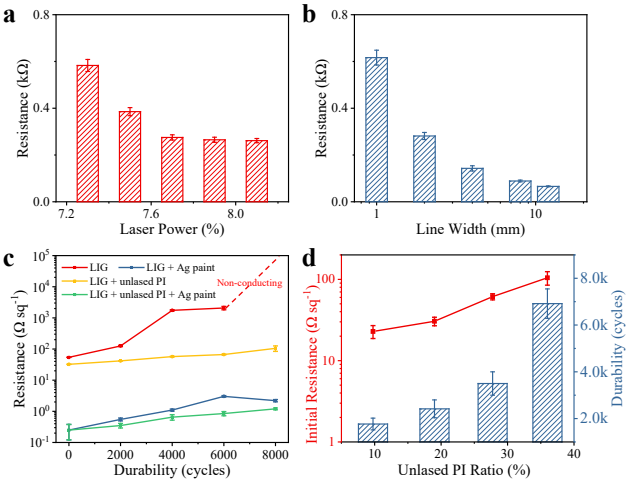

***Figure 2**: Parameter optimization of (a-b) device electrodes and (c-d) via interconnection.*

When the minimum power of the laser inducing is less than 7.3% (threshold), the formed LIG network is discontinuous and insufficient. After exceeding the threshold, the resistance of the LIG film gradually decreases and tends to be saturated (Fig. 2(a)). However, the thickness of the LIG film will continue to increase, making it easy to delaminate. The influence of laser power on the quality of LIG formation is greater than the scanning rate of the laser. By adjusting the line width, the corresponding resistance can be well controlled (Fig. 2(b)). In addition to the unlased PI that largely buffers the mechanical impact on the via, silver paint (SPI Supplies, Inc.) further enhances via's conductivity (Fig. 2(c)). Besides, Fig. 2(d) describes that the unlased PI ratio of 20% is relatively effective for the good conductivity and durability.

Active sensing performance of LIG-TENG

Fig. 3(a) reveals the working principle of LIG-TENG on the inner side of the smart bracelet. When worn on the wrist, LIG-TENG will continue to rub against the skin accompanied by limb motions. One material captures electrons from the other due to the difference in electron affinity at the interface. In this work, polytetrafluoroethylene (PTFE) serves as the friction layer due to its strong electronegativity. Every time the skin approaches the inner side of the bracelet, it will cause the induced charge on the LIG, resulting in a potential output. It is worth noting that each arm swing motion will trigger two obvious skin-device contact-separation processes, thereby two pulsed output represents an arm swing cycle (Fig. 3(b)). We can use the signal frequency to obtain real-time motion information in different exercise states of the body (Fig. 3(c)).

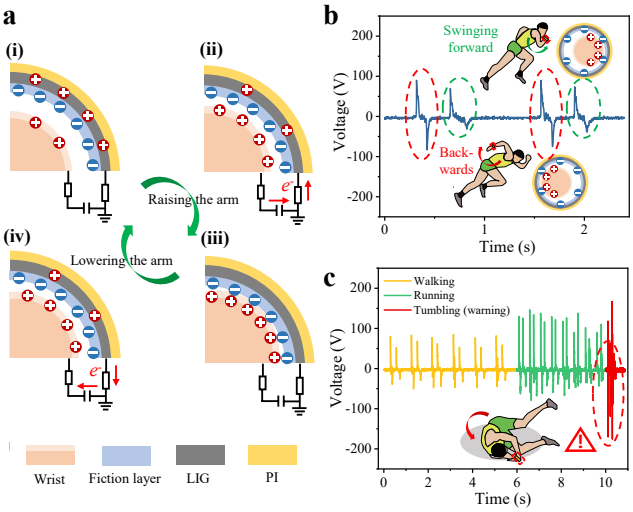

***Figure 3**: (a) Schematic diagram and (b) Signal generation of LIG-TENG as an active sensor. (c) Signal output of LIG-TENG in different motion states.*

Since the arm swing strength and amplitude are more obvious during running motions, we can match them with the output amplitude of LIG-TENG, so as to obtain more abundant detection parameters. Moreover, a sudden tumble during outdoor sports will spark abnormal signal output of LIG-TENG (Fig. 3(c)). Through this real-time and reliable information, we could carry out first-hand danger warning and timely treatment.

Energy harvesting performance of LIG-TENG

In addition to the aforementioned sensing role played in human movements, LIG-TENG can also collect the

steady stream of kinetic energy in human leisure time. Figure 4 (a-b) show the open-circuit voltage (V_{oc}) and short-circuit current (I_{sc}) of the LIG-TENG at different swing arm frequencies, respectively, from which the peak voltage outputs basically reach one hundred volts, and the current outputs are in the range of tens of microamperes. To further characterize its ability to collect kinetic energy, we measure the voltages and powers under a series of different load resistance (Fig. 4(c)), with a swing frequency of 2 Hz for actuation. With a load resistance of 1 megohms, the LIG-TENG reaches a maximum power output of 1.296 mW. In addition, after more than 20,000 cycles of stability testing, the degradation of LIG-TENG performance is negligible (Fig. 4(d)).

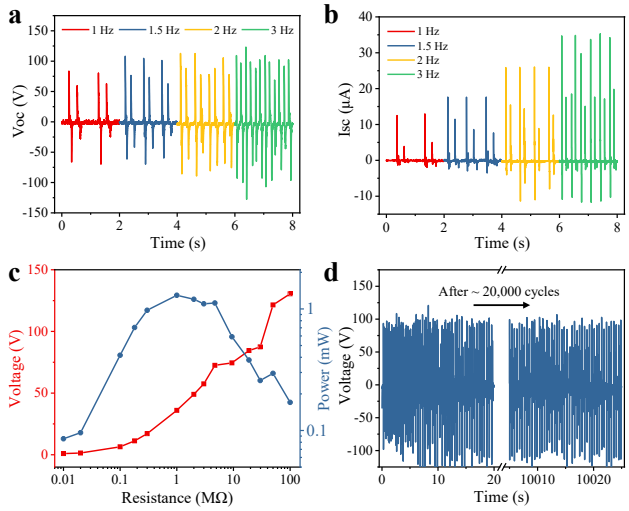

***Figure 4**: LIG-TENG for collecting human kinetic energy: (a) V_{oc} and (b) I_{sc} of the device at different frequencies, (c) matching impedance test, and (d) cycle stability test.*

Energy Storage performance of LIG-MSCs

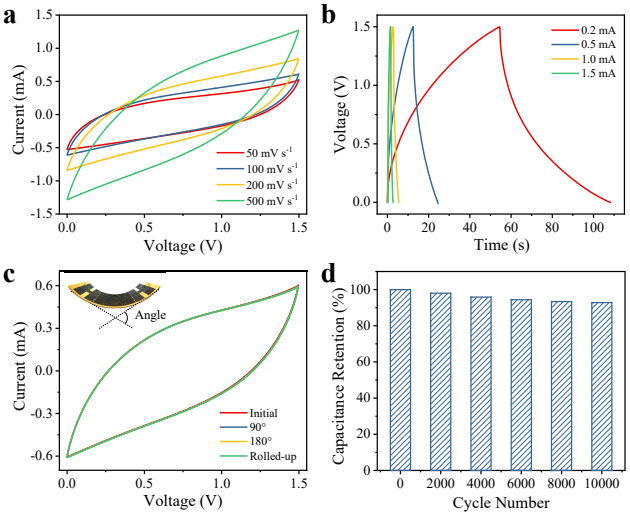

***Figure 5**: (a-b) Electrochemical performance and (c) Mechanical tolerance test and (d) Long-term durability test of single LIG-MSC.*

With regard to the in-situ energy storage capacity of the LIG-MSCs, we first characterize the electrochemical performance of single LIG-MSC through cyclic voltammetry (CV), galvanostatic charging/discharging tests (GCD), mechanical stability as well as cycling stability tests. The CV curves with quasi-rectangular shapes observed in Fig. 5(a) indicate the good electrochemical activity of LIG interdigital electrodes. Interestingly, the CV windows can reach 1.5V (supply potential of traditional batteries) without localized breakdown effect, which is attributed to the fine and uniform laser assisted processing. The GCD test in Fig. 5(b) visually reflects the charging/discharging processes of LIG-MSC. The quasi-linear voltage-time profiles profit from the effective channels for ion transport provided by LIG network. Besides, the mechanical tolerance test (Fig. 5(c)) and long-term durability test (Fig. 5(d)) demonstrates the excellent mechanical and electrical properties of LIG electrodes, respectively.

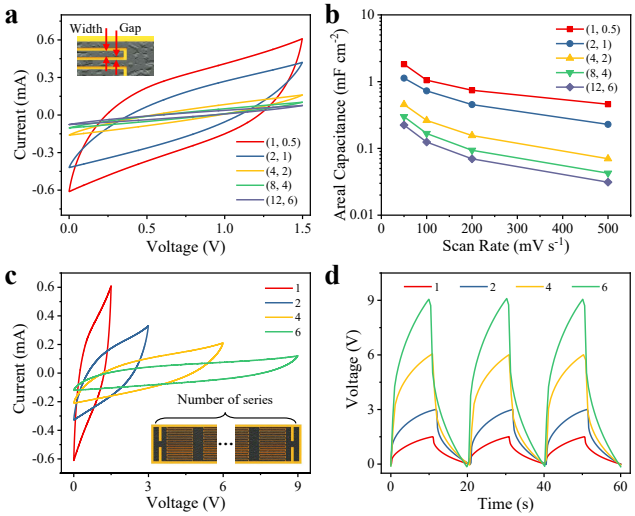

***Figure 6**: (a-b) Parameter optimization and (c-d) Series design of LIG-MSC.*

Furthermore, in order to better realize the energy transfer matching between LIG-TENG and LIG-MSC, we optimize the design of LIG-MSC. Firstly, we analyzed the influence of electrode width and electrode gap on the performance (Fig. 6(a-b)). It can be clearly seen that the density of the electrodes determines the capacitance between the electrodes. Considering the influence of the electrode width on the initial resistance, the electrode width of the final prepared LIG-MSC is 1 mm and the spacing is 500 μm. Secondly, the series design can effectively broaden the potential window (Fig. 6(c)) and achieve a higher storage voltage under the same current input (Fig. 6(d)), which allows us to select appropriate number of series to meet the voltage standard of the driving electronics.

Performance of sensing & energy system

The block diagram of Fig. 7(a) uncovers the working modes of the whole smart bracelet. The outputs of the inner LIG-TENG could not only serve as active sensing to reflect the physiological state of the human body, but also be stored in the outer LIG-MSCs in the form of energy. Double-sided devices are assembled into a SCPU, which can apply to process and transmit the active signals as well as directly drive low-power electronic equipment.

The self-charging capacity of SCPU is reflected in Fig. 7(b). In the actual running process, the SCPU composed of six LIG-MSCs in series can be charged to 0.3 V less than ten

minutes. Moreover, there is no trend of saturation in the charging voltage, indicating that the SCPU can continue to harvest human motion energy.

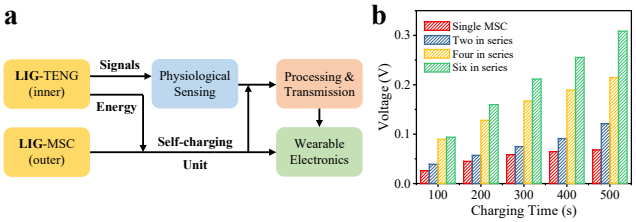

***Figure 7**: (a) Working block diagram of the smart bracelet and (b) Performance of the LIG-based self-charging unit.*

CONCLUSIONS

In summary, we present a smart bracelet system based on double-sided LIG technology that integrates active sensing, energy harvesting and energy storage. The high conductivity and large-area preparation of LIG enable the formed TENG to efficiently convert human motion energy into sensing signals and power output. LIG-MSCs based on high surface area interdigital electrodes deliver admirable electrochemical performance. Furthermore, the SCPU formed by via interconnection with optimized design shows great potential in powering the wearable electronics.

ACKNOWLEDGEMENTS

This work was supported by National Key R&D Project from Minister of Science and Technology, China (2016YFA0202701, 2018YFA0108100) and the National Natural Science Foundation of China (Grant No. 61674004).

REFERENCES

[1] J. Wan, H. Wang, L. Miao, X. Chen, Y. Song, H. Guo, C. Xu, Z. Ren, and H. Zhang, "A flexible hybridized electromagnetic-triboelectric nanogenerator and its application for 3D trajectory sensing", *Nano Energy*, vol. 74, pp. 104878, 2020.

[2] H. Wang, Y. Song, L. Miao, J. Wan, X. Chen, X. Cheng, H. Guo, and H. Zhang, "Stamp-assisted gravure printing of micro-supercapacitors with general flexible substrates", *32nd IEEE MEMS*, Seoul, Korea, January 27-31, 2019, pp. 950-953.

[3] H. Guo, J. Wan, H. Wu, H. Wang, L. Miao, Y. Song, H. Chen, M. Han, and H. Zhang, "Self-powered multifunctional electronic skin for a smart anti-counterfeiting signature system", *ACS Appl. Mater. Inter.*, vol. 12, pp. 22357-22364, 2020.

[4] Y. Song, J. Min, Y. Yu, H. Wang, Y. Yang, H. Zhang, and W. Gao, "Wireless battery-free wearable sweat sensor powered by human motion", *Sci. Adv.*, vol. 6, pp. eaay9842, 2020.

[5] Y. Yang, Y. Song, X. Bo, J. Min, O.S. Park, L. Zhu, M. Wang, J. Tu, et al., "A laser-engraved wearable sensor for sensitive detection of uric acid and tyrosine in sweat", *Nat. Biotechnol.*, vol. 38, pp. 217-224, 2020.

[6] X. Chen, Z. Ren, H. Guo, X. Cheng, and H. Zhang, "Self-powered flexible and transparent smart patch for temperature sensing", *Appl. Phys. Lett.*, vol. 116, pp. 043902, 2020.

[7] Z. Ren, Q. Zheng, H. Wang, H. Guo, L. Miao, J. Wan, C. Xu, S. Cheng, and H. Zhang, "Wearable and self-cleaning hybrid energy harvesting system based on micro/nanostructured haze film", *Nano Energy*, vol. 67, pp. 104243, 2020.

[8] Y. Song, H. Wang, X. Cheng, G. Li, X. Chen, H. Chen, L. Miao, X. Sheng, and H. Zhang, "High-efficiency self-charging smart bracelet for portable electronics", *Nano Energy*, vol. 55, pp. 29-36, 2019.

[9] K. Dong, X. Peng, J. An, A.C. Wang, J. Luo, B. Sun, J. Wang, and Z.L. Wang, "Shape adaptable and highly resilient 3D braided triboelectric nanogenerators as e-textiles for power and sensing", *Nat. Commun.*, vol. 11, pp. 1-11, 2020.

[10] H. Wang, Y. Song, H. Guo, J. Wan, L. Miao, C. Xu, Z. Ren, X. Chen, and H. Zhang, "A three-electrode multi-module sensor for accurate bodily-kinesthetic monitoring", *Nano Energy*, vol. 68, pp. 104316, 2020.

[11] X. Chen, Y. Song, H. Chen, J. Zhang, and H. Zhang, "An ultrathin stretchable triboelectric nanogenerator with coplanar electrode for energy harvesting and gesture sensing", *J. Mater. Chem. A*, vol. 5, pp. 12361-12368, 2017.

[12] H. Guo, H. Wu, Y. Song, L. Miao, X. Chen, H. Chen, Z. Su, M. Han, and H. Zhang, "Self-powered digital-analog hybrid electronic skin for noncontact displacement sensing", *Nano Energy*, vol. 58, pp. 121-129, 2019.

[13] X.S. Zhang, M. Han, B. Kim, J.F. Bao, J. Brugger, and H. Zhang, "All-in-one self-powered flexible microsystems based on triboelectric nanogenerators", *Nano Energy*, vol. 47, pp. 410-426, 2018.

[14] H. Chen, Y. Song, X. Cheng, and H. Zhang, "Self-powered electronic skin based on the triboelectric generator", *Nano Energy*, vol. 56, pp. 252-268, 2019.

[15] C. Chen, H. Guo, L. Chen, Y.-C. Wang, X. Pu, W. Yu, F. Wang, Z. Du, and Z.L. Wang, "Direct current fabric triboelectric nanogenerator for biomotion energy harvesting", *ACS Nano*, vol. 14, pp. 4585-4594, 2020.

[16] X. Shi, S. Chen, H. Zhang, J. Jiang, Z. Ma, and S. Gong, "Portable self-charging power system via integration of a flexible paper-based triboelectric nanogenerator and supercapacitor" *ACS Sustainable Chem. Eng.*, vol. 7, pp. 18657-18666, 2019.

[17] J. Lin, Z. Peng, Y. Liu, F. Ruiz-Zepeda, R. Ye, E.L.G. Samuel, M.J. Yacaman, B.I. Yakobson, and J.M. Tour, "Laser-induced porous graphene films from commercial polymers", *Nat. Commun.*, vol. 5, pp. 1-8, 2014.

CONTACT

*H.X. Zhang, hxzhang@pku.edu.cn